BUDAPEST UNIVERSITY OF TECHNOLOGY AND ECONOMICS
FACULTY OF MECHANICAL ENGINEERING
DEPARTMENT OF MACHINE AND PRODUCT DESGIN
GÉZA PATTANTYÚS-ÁBRAHÁM DOCTORAL SCHOOL OF MECHANICAL ENGINEERING SCIENCES

Development of the Loading Model for a Hip-Region Reconstruction Implant

Booklet of New Scientific Results

Authored by:
Martin Olivér Dóczi
MSc in Mechanical Engineering

Supervisor:
Péter Tamás Zwierczyk, PhD
Assistant Professor

Budapest, 2025

1. Introduction

Hip osteoarthritis is one of the major widespread diseases of our time, with sedentary lifestyle and obesity recognized as significant risk factors [Lespasio2018]. Due to increased life expectancy and the growing demand for a pain-free quality of life, the need for total hip replacement is emerging in an increasing number of individuals, and at younger ages (*Figure 1*).

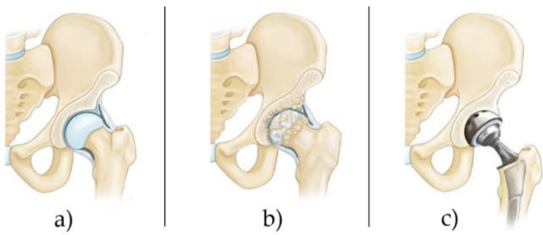

Figure 1 Clinical conditions of the hip joint: healthy (a); affected by osteoarthritis (b); treated with total hip replacement (c) [Orthoinfo2020]

In parallel, the number of revision surgeries—procedures involving the replacement, removal, or re-implantation of previously implanted hip components—is also on the rise. These revision procedures increasingly encounter extensive pelvic bone defects (*Figure 2*) [Paprosky1994], [Bejek2013].

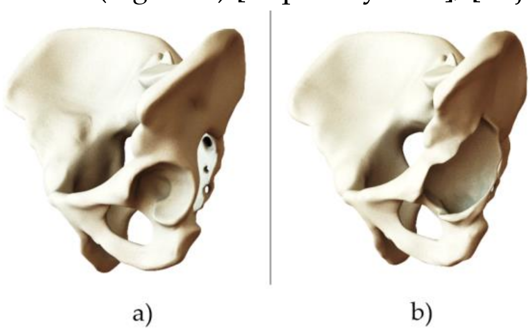

Figure 2 Healthy pelvis (a) and extensive acetabular bone loss (b)

Over the years, the previously implanted acetabular component tends to migrate in a superior-medial direction, leading to bone resorption and a significant displacement of the hip joint's center of rotation from its original anatomical position.

Treating this condition poses a major challenge—not only from a medical but also from an engineering perspective. One possible treatment option is the use of an acetabular reinforcement cage, which is anchored to the remaining intact regions of the pelvis via fixation flanges, and serves to restore the original center of rotation [Ahmad2015].

To fill the defect behind the cage, either porous metal augments or bone grafts are used. In the latter case, there is a potential for the graft to integrate and transform into living bone tissue, once again becoming part of the pelvic structure. *Figure 3* shows an acetabular reinforcement using a cage and bone grafts to fill the defect.

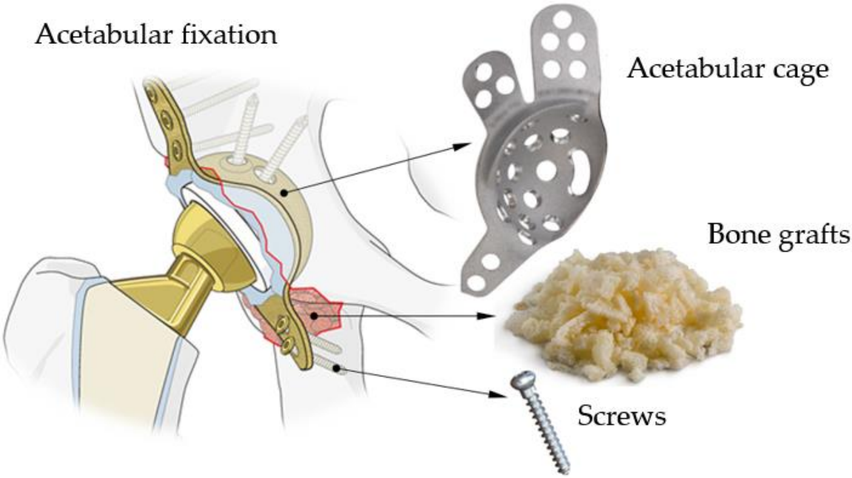

Figure 3 Main parts of an acetabular replacement [AO], [Saumya], [Crockrarell2009], [Param]

From an engineering perspective, the design of such implants presents challenges on multiple fronts. In terms of geometry, there is significant individuality not only in the patient's anatomical structure but also in the morphology of the bone defect itself. This implies that the design space available for the fixation flanges can vary greatly between patients, and currently, no standardized guidelines exist in the literature.

Another challenge lies in the material properties of both the bone and the grafts used to fill the defect. These properties cannot be confined to narrow intervals and, moreover, behave as living materials—their structure may change over time due to mechanical and biological effects. As such, the implant must operate in a highly uncertain and temporally variable material environment.

The loading conditions in the hip joint also vary considerably depending on the patient's body type and lifestyle. These loads show a wide diversity in both magnitude and direction. Due to their number and variability, determining representative loading scenarios for implant design is itself a complex task.

Despite these challenges, from the patient's perspective, it is highly desirable to realize an implant that—while customized—is also mechanically reliable (i.e., with low risk of failure), and that, due to its compliant nature, supports the integration and biological incorporation of bone grafts.

My research focuses on the design of customized pelvic reconstruction implants (acetabular cages), with particular attention to the modeling of forces acting in the hip joint. My objective is to incorporate physiologically relevant forces—whose general magnitude, characteristics, and relative frequency are available in the literature—into the design process using computational models. These models must serve both mechanical integrity (implant strength) and biomechanical functionality, particularly the promotion of graft-to-bone incorporation [Mirulla2021].

This includes the development of methodologies or algorithms capable of estimating patient-specific loading conditions based on available (measured or modeled) joint forces. The goal is to enable more effective, individualized design of acetabular cages.

The anticipated impact of the research and the formulated theses is to facilitate the design of such customized implants. By enabling efficient and cost-effective finite element simulations for design validation or optimization, the process becomes more accessible and clinically applicable.

2. Background and Research Methods

The clinical demand that defined the direction of this research originated from Dr. Róbert Sződy, Chief Orthopaedic and Trauma Surgeon. In his work and that of his collaborators, custom-made sheet metal acetabular cages were applied [Sződy2017].

For my work, I utilized tools of biomechanical finite element modeling, which are well-established in the literature. The literature review comprehensively covered relevant anatomical, clinical, and biomechanical aspects. Regarding the latter, the focus was placed primarily on pelvic loading conditions and the modeling of bone and bone graft remodeling processes.

A particularly important reference in the field is the work of Bergmann et al. [Bergmann2001], who conducted in vivo measurements of physiological hip joint loads in multiple patients. These measurements were expressed as a percentage of body weight, and average patterns were published. These fundamental daily activity-related load cases formed the backbone of my research. While these loading scenarios have been widely adopted in the literature, accounting for all of them in detail is computationally demanding. Therefore, it is necessary to reduce the number of required simulations by defining representative or surrogate loads.

It is also important to note that surrogate loads used for strength assessment differ in nature from those used in the modeling of bone graft remodeling processes.

In the literature, strength assessment of hip-related implants has received more emphasis. Publications addressing this aspect consistently relied on the selection of a subset of daily activity loads—typically including the peak joint force during walking and stair climbing [Bergmann2001], [Costin2014], [Plessers2016], [Totoribe2018]. Some studies considered additional activities, but the common approach involved manual selection of representative load cases. This poses a limitation, as such selection does not account for smaller but directionally distinct forces, which also occur in the hip joint and can critically affect mechanical integrity.

To address this, I developed and implemented a deterministic algorithm that generates loading vectors around which no greater load occurs. This allows for more reliable strength assessments across the entire relevant load space.

In contrast, modeling bone graft remodeling presents a fundamentally different challenge. While biological factors undoubtedly influence the remodeling process, this research focuses solely on the mechanical loading aspects and their modeling.

Under mechanical loads, adaptive processes are initiated within the graft, which can be modeled in finite element simulations by modifying material properties over time. Literature commonly relates these adaptive changes to the distribution of strain energy density resulting from so-called pseudo-loads [Mirulla2021]. The role of pseudo-loads is to replace the complex, multiaxial, cyclic real-world load history with simplified loading conditions. This is necessary because it is impractical to model the graft state after every walking step.

Each type of daily activity generates a large number of cycles with varying magnitudes and directions, so their mechanical impact must be aggregated, also considering their relative frequency. Pseudo-loads therefore represent the accumulated effect of repeated loading over a given time interval.

Using pseudo-loads, strain energy density is calculated for each finite element. This value is then divided by the element's apparent density, defined over its current volume, which also characterizes the stiffness of the graft as a spatial domain. The resulting value, known as the stimulus, determines the local remodeling behavior: underload or overload leads to resorption (reduction in density and stiffness), optimal loading leads to reinforcement (increase in density and stiffness), and no significant change occurs in the so-called "lazy zone."

A mechanical derivation confirms that these pseudo-loads depend only on the external loading conditions. Using iterative simulations under these loads, the time-dependent transformation of the bone graft can be modeled in a finite element framework. Of course, the application of relevant constraints—such as linear material behavior and the requirement for a common origin of the load vectors—is essential, and these are reflected in the related thesis points.

3. Summary of the Research

The research is centered around biomechanical finite element modeling, a multidisciplinary field encompassing numerous thematic areas.

As a first step, I reviewed the relevant anatomical and clinical literature to gain an understanding of the structural characteristics of the pelvis with bone defects and the treatment strategies applied in such cases.

A key element of the research was the development of a finite element model that strikes a balance between sufficient anatomical and mechanical detail and computational feasibility—ensuring that simulations remain executable on standard personal computers. In addition, the model was required to provide qualitatively accurate results regarding the load-bearing behavior of the acetabular cage and its surrounding structures. In other words, the goal was to create a validated finite element model.

For this purpose, patient-specific CT (Computed Tomography) datasets were available from both immediate postoperative and one-year follow-up scans.

From the biomechanical literature, detailed methodologies were available regarding the development of such finite element models. However, a critical revision of these methods was necessary for validation purposes. Based on the literature and my own methodological considerations, I published a finite element model suitable for implant analysis [Dóczi2020a].

A standard validation approach in the literature is to test the model under peak hip joint loading during walking. Applying this to multiple patients, the model consistently predicted failure in the same zone where fractures were later observed in the actual implants. This correlation was confirmed using follow-up CT data from the patients.

While this validation approach provided a solid foundation, it only covered a narrow segment of the full spectrum of daily activity loads. Therefore, I proposed a new conceptual approach: instead of selecting individual load cases based on their magnitude or frequency, strength evaluations should be carried out for load vectors that have no higher magnitude load occurring within a small conical neighborhood around them. I termed these vectors as major loads (*Figure 4*).

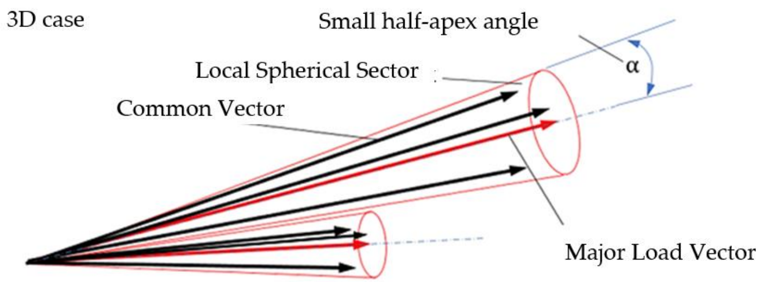

Figure 4 Explanation of major loads

This approach does not require any modification to the commonly used loading and boundary condition definitions in the literature; rather, it involves the consideration of additional, previously unaccounted-for load cases.

In this context, determining representative loads formally requires a geometric coverage of the full 3D daily activity load vector space using as few spherical caps of a given half-apex angle as possible. A characteristic of such geometric covering problems is that no known polynomial-time algorithm exists to solve them. In other words, these problems are NP-hard—their solutions can be verified in polynomial time, but cannot necessarily be found in polynomial time.

To produce a deterministic solution, I developed a heuristic algorithm tailored to the problem, which successfully covered the loading vector space with 10 spherical caps, each having a 10° half-apex angle.

When visualizing the load vectors from the literature in the context of this spherical cap approach, it becomes evident that many high-magnitude, directionally distinct, and not infrequent loading scenarios are not subjected to strength verification [Dóczi2023b].

Comparing the finite element model stress results under conventional literature-based load vectors and under the newly introduced principal loading directions showed that while the high-stress concentration zones identified under standard loading conditions are preserved, additional potential failure regions are revealed under the new loading conditions. Thus, the new method does not contradict prior results but rather extends and enhances them. Strength verification can therefore be carried out more comprehensively, while the increase in computational cost remains moderate: using 10 representative load vectors instead of 9 standard activity peaks provides a more complete assessment for the average patient [Dóczi2023b].

Bone grafts located behind the acetabular cage adapt structurally in response to mechanical stimuli, particularly those related to strain energy density. Since simulating the full spectrum of daily activities is computationally expensive, I proposed a surrogate loading method to reduce simulation costs [Dóczi2023a].

Using mechanical formulations and literature-based load vectors—defined with a common origin and associated relative frequencies—I applied a linear model to calculate the average distribution of strain energy density over all loading conditions. From the matrix constructed from these external loads, three surrogate loading vectors can be derived, which, when averaged, yield identical strain energy density distributions as the full load set.

The method was validated using a finite element model of a bone graft positioned behind an acetabular cage [Dóczi2023a]. The surrogate loading vectors can be computed in closed form, and simulations show that they reproduce the reference model's energy density distribution within numerical tolerance on each iteration—demonstrating the method's efficiency and accuracy.

4. New Scientific Results

The first new scientific result presents an algorithm that provides a spherical cap-based coverage of daily activity-related load vectors.

First new scientific result [Dóczi2023b]

In three-dimensional space, a set of vectors originating from a common point can be covered by spherical caps with an arbitrarily chosen half-apex angle, using the following algorithm: In the first phase, the input 3D vectors are normalized to unit vectors, the central directions of the spherical caps—i.e., the major loading directions—are determined. In the second phase, the magnitudes of these major load vectors are set accordingly (*Figure 5*).

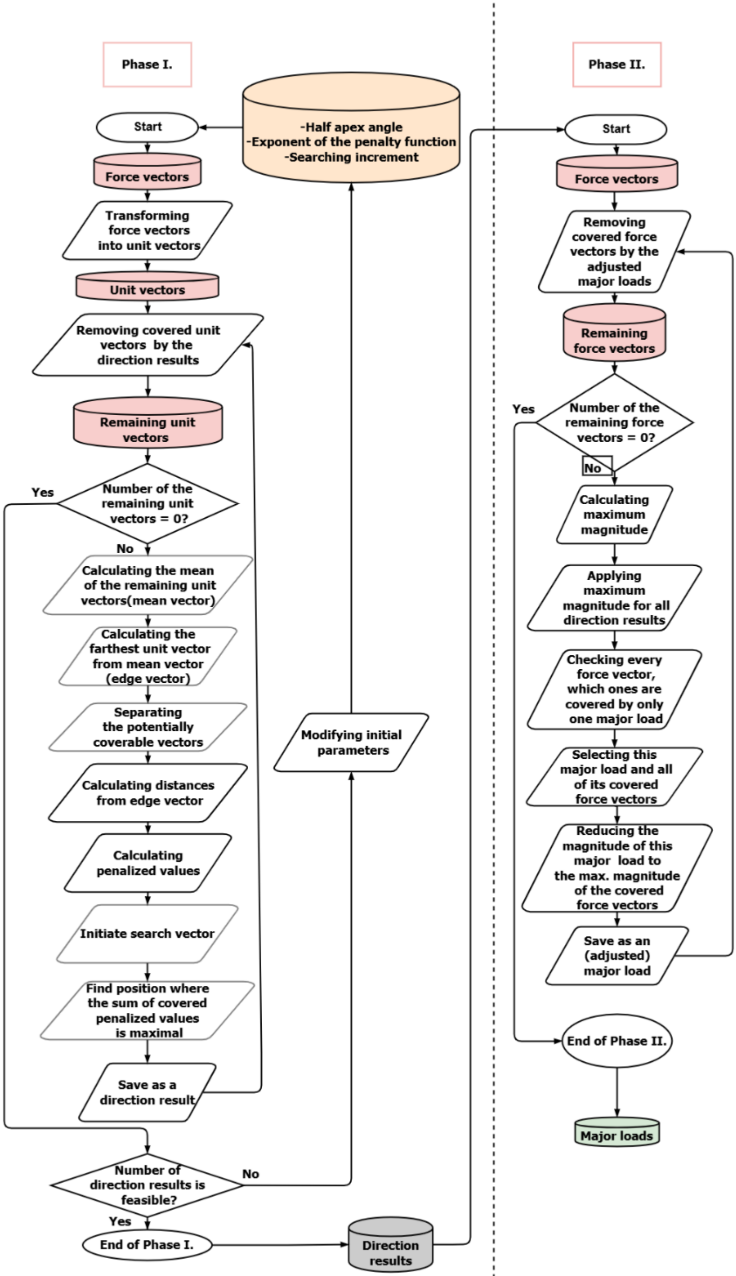

Figure 5 **Flowchart for calculating principal loading directions from 3D load vectors**

The second new scientific result defines the loading and boundary condition specifications required for the finite element–based static strength analysis of acetabular cages.

<u>**Second new scientific result**</u> **[Dóczi2018], [Dóczi2020a], [Dóczi2022], [Dóczi2023b]**

For the finite element–based static strength analysis of acetabular cages used in the treatment of bone defects without pelvic discontinuity, the following boundary and loading conditions must be applied:

- **Boundary conditions: On the hemi-pelvic model with bone defect, fixed constraints shall be applied at the articular surface of the pubic symphysis and at the sacroiliac joint interface**
- **Loading conditions: Ten distinct load vectors—each acting as a force applied at the center of rotation of the hip joint—shall be defined individually these vectors are expressed in terms of body weight percentage [BW%]:**

Table 1 Suggested major loads

#	***x* component [BW%]**	***y* component [BW%]**	***z* component [BW%]**
1	**66,15**	**66,18**	**243,39**
2	**42,19**	**-71,89**	**237,65**
3	**60,62**	**-44,67**	**233,17**
4	**35,41**	**11,99**	**240,21**
5	**98,18**	**16,14**	**191,44**
6	**40,90**	**-121,47**	**173,46**
7	**90,51**	**-128,20**	**108,11**
8	**69,16**	**-62,23**	**119,74**
9	**63,56**	**-18,18**	**92,72**
10	**34,89**	**-38,78**	**23,17**

In this right-handed coordinate system, the x-axis is defined by the line connecting the centers of rotation of the hip joints and points inward, into the pelvis. The z-axis is perpendicular to the x-axis and passes through the center of the sacrum, pointing superiorly. The y-axis is defined as perpendicular to both the x- and z-axes [Bergmann2001].

The third new scientific result presents the calculation of surrogate loading vectors for modeling bone graft remodeling. These vectors are derived through mechanical formulations and serve to replicate the effect of strain energy density, which is known to drive graft transformation.

Third new scientific result [Dóczi2020b], [Dóczi2021], [Dóczi2023a], [Dóczi2023c]

If a structure is subjected to multiple force load cases that converge at a common node, and these loads can be grouped into load sets, where the average strain energy density within each set is computed through simple averaging—and the overall mean is obtained as a weighted average of these sets (with weight factors summing to 1)—then, under the assumption of a linear finite element model, it is possible to derive, in closed form, three equivalent load vectors which arithmetic mean of the strain energy densities induced by these equivalent vectors is, within numerical tolerance, equivalent to the weighted average strain energy density distribution generated by the full set of loads by the following:

$$\underline{\underline{\Phi}} = \begin{bmatrix} \Phi_{11} & \Phi_{12} & \Phi_{13} \\ \Phi_{12} & \Phi_{22} & \Phi_{23} \\ \Phi_{13} & \Phi_{23} & \Phi_{33} \end{bmatrix} =$$

$$= \begin{bmatrix} 3 \cdot \sum_{i=1}^{n} \frac{w_i}{k_i} \cdot \sum_{j=1}^{k_i} a_{ij}^2 & 3 \cdot \sum_{i=1}^{n} \frac{w_i}{k_i} \cdot \sum_{j=1}^{k_i} a_{ij} \cdot b_{ij} & 3 \cdot \sum_{i=1}^{n} \frac{w_i}{k_i} \cdot \sum_{j=1}^{k_i} a_{ij} \cdot c_{ij} \\ 3 \cdot \sum_{i=1}^{n} \frac{w_i}{k_i} \cdot \sum_{j=1}^{k_i} a_{ij} \cdot b_{ij} & 3 \cdot \sum_{i=1}^{n} \frac{w_i}{k_i} \cdot \sum_{j=1}^{k_i} b_{ij}^2 & 3 \cdot \sum_{i=1}^{n} \frac{w_i}{k_i} \cdot \sum_{j=1}^{k_i} b_{ij} \cdot c_{ij} \\ 3 \cdot \sum_{i=1}^{n} \frac{w_i}{k_i} \cdot \sum_{j=1}^{k_i} a_{ij} \cdot c_{ij} & 3 \cdot \sum_{i=1}^{n} \frac{w_i}{k_i} \cdot \sum_{j=1}^{k_i} b_{ij} \cdot c_{ij} & 3 \cdot \sum_{i=1}^{n} \frac{w_i}{k_i} \cdot \sum_{j=1}^{k_i} c_{ij}^2 \end{bmatrix}, \quad (1)$$

where,

$\underline{\underline{\Phi}}$: A symmetric matrix constructed from the components, number, and relative frequencies of the external force vectors,

n : Number of load groups,

i : Index of the load groups,

j : Index of individual load vectors within a load group,

w_i : Weight factor of the i-th load group ($\sum_{i=1}^{n} w_i = 1$),

k_i : Number of load vectors in the i-th load group,

a : x direction component,

b : y direction component,

c : z direction component,

The equivalent load vectors are to be determined in the following form:

$$\underline{f}_{subst,1} = \begin{bmatrix} a_{subst,1} \\ 0 \\ 0 \end{bmatrix}; \underline{f}_{subst,2} = \begin{bmatrix} a_{subst,2} \\ b_{subst,3} \\ 0 \end{bmatrix}; \underline{f}_{subst,3} = \begin{bmatrix} a_{subst,3} \\ b_{subst,3} \\ c_{subst,3} \end{bmatrix}, \quad (2)$$

where,

$\underline{f}_{subst}$: A vector constructed from the components of the equivalent load,

a from which the required force vector can be expressed as a linear combination of the unit load vectors in the x, y, and z directions as follows:

$$\underline{\boldsymbol{F}}_{subst,p} = \boldsymbol{a}_{subst,p} \cdot \underline{\boldsymbol{F}}^{(x)}_{unit} + \boldsymbol{b}_{subst,p} \cdot \underline{\boldsymbol{F}}^{(y)}_{unit} + \boldsymbol{c}_{subst,p} \cdot \underline{\boldsymbol{F}}^{(z)}_{unit}, \quad (3)$$

where,

p : Index of the equivalent load vectors (p =1,2,3),

$\underline{\boldsymbol{F}}_{unit}$: Unit load vector in the respective direction,

The components of the equivalent load vectors can be computed as follows, interpreting the indeterminate form 0/0 as zero:

$$\boldsymbol{c}_{subst,3} = \sqrt{\boldsymbol{\Phi}_{33}}, \quad (4)$$

$$\boldsymbol{b}_{subst,3} = \frac{\boldsymbol{\Phi}_{23}}{\boldsymbol{c}_{subst,3}}, \quad (5)$$

$$\boldsymbol{a}_{subst,3} = \frac{\boldsymbol{\Phi}_{13}}{\boldsymbol{c}_{subst,3}}, \quad (6)$$

$$\boldsymbol{b}_{subst,2} = \sqrt{\boldsymbol{\Phi}_{22} - \boldsymbol{b}^2_{subst,3}}, \quad (7)$$

$$\boldsymbol{a}_{subst,2} = \frac{\boldsymbol{\Phi}_{12} - \boldsymbol{a}_{subst,3} \cdot \boldsymbol{b}_{subst,3}}{\boldsymbol{b}_{subst,2}}, \quad (8)$$

$$\boldsymbol{a}_{subst,1} = \sqrt{\boldsymbol{\Phi}_{11} - -\boldsymbol{a}^2_{subst,2} - \boldsymbol{a}^2_{subst,3}}. \quad (9)$$

5. Practical Application of the Results

The algorithm presented as the first new scientific result can also be used to determine major loading directions for other load distributions and with different half-apex angles. For example, it may be applied to patient-specific hip joint force datasets obtained via inverse kinematic methods. Similarly, it can be used for the structural verification of other comparably loaded systems.

The loading and boundary conditions proposed in the second new scientific result for static elastic strength analysis are defined as body-weight-percentage-based loads for an average patient, and are immediately applicable for the verification of various implant designs.

As described in the third new scientific result, the average strain energy density distribution arising from multiple load cases, weighted by their relative frequency, can be approximated by averaging the results of simulations using only three equivalent load vectors. This approach enables cost-effective prediction of bone–bone graft remodeling, and it also supports comparative analysis of different loading spectra, which is useful for parameter estimation of the material properties driving graft transformation.

6. References

List of the Author's Publications

[Dóczi2018] M. O. Dóczi, J. Simonovics, "Egyedi vápakosaras rögzítés végeselemes modelljének elkészítése," GÉP, vol. 2018, no. 3, pp. 8-11, 2018.

[Dóczi2020a] M. O. Dóczi, R. Sződy, P. T. Zwierczyk, "Failure analysis of a custom made acetabular cage with finite element method," in Proceedings of the 34th International ECMS Conference on Modelling and Simulation (eds. M. Steglich, C. Mueller, G. Neumann, M. Walther), Communications of the ECMS, vol. 34, no. 1, Wildau, Germany, June 2020, pp. 250-255, DOI: http://doi.org/10.7148/2020.

[Dóczi2020b] M. O. Dóczi, R. Sződy, P. T. Zwierczyk, "Csontgraft változásának végeselemes modellezése HyperMesh-Calculix környezetben," GÉP, vol. 2020, no. 7-8, pp. 15-18, 2020.

[Dóczi2021] M. O. Dóczi, R. Sződy, P. T. Zwierczyk, "Implementation of bone graft adaptation's FE model in HyperMesh," in Proceedings of the 35th International ECMS Conference on Modelling and Simulation (eds. Khalid Al-Begain, Mauro Iacono, Lelio Campanile, Andrzej Bargiela), Communications of the ECMS, vol. 35, no. 1, Web-organised Conference, June 2021, DOI: https://doi.org/10.7148/2021-0152.

[Dóczi2022] M. O. Dóczi, R. Sződy, P. T. Zwierczyk, "Effect of the Design Constraints and the Loading Model on the Geometry of Topology Optimized Acetabular Cages", Periodica Polytechnica Mechanical Engineering, vol. 66, no. 3, pp. 253–259, 2022.
Available at: https://doi.org/10.3311/PPme.20238.

[Dóczi2023a] M. O. Dóczi, R. Sződy, P. T. Zwierczyk, "Equivalent loads from the life-cycle of acetabular cages in relation to bone-graft transformation," Computer Methods and Programs in Biomedicine, vol. 236, p. 107654, 2023.
Available at: https://doi.org/10.1016/j.cmpb.2023.107564.

[Dóczi2023b] M. O. Dóczi, R. Sződy, P. T. Zwierczyk, "Extended mechanical loads for the analysis of acetabular cages," Biomechanics and Modeling in Mechanobiology, vol. 22, pp. 1411–1423, 2023.
Available at: https://doi.org/10.1007/s10237-023-01728-z.

[Dóczi2023c] M. O. Dóczi, P. T. Zwierczyk, "Topology optimization with displacement constraints: a comparative analysis of acetabular cage designs and bone graft's strain energy density," Biomechanica Hungarica, vol. 16, no. 1, pp. 7–16, 2023.
Available at: https://doi.org/10.17489/biohun/2023/1/582.

List of References

[Ahmad2015] A. Ahmad, R. Schwarzkopf, "Clinical evaluation and surgical options in acetabular reconstruction: A literature review," J. Orthop., vol. 12, no. 2, pp. S238–S243, 2015. [Online]. Available at: https://doi.org/10.1016/j.jor.2015.10.011.

[Bejek2013] Z. Bejek, J. Lakatos, M. Szendrői, "Váparekonstrukciós lehetőség kiterjedt os ilii defektus esetén revíziós műtétekben," 2013. [Online]. Available at: https://matrokplaszt.files.wordpress.com/2014/08/04-bejek2.pdf. [Accessed on: 2023.09.14. 14:58].

[Bergmann2001] G. Bergmann, G. Deuretzbacher, M. Heller, F. Graichen, A. Rohlmann, J. Strauss, G. Duda, "Hip contact forces and gait patterns from routine activities," J. Biomech., vol. 34, no. 7, pp. 859–891, 2001. [Online]. Available at: https://doi.org/10.1016/S0021-9290(01)00040-9.

[Costin2014] S. Costin, C. Micu, S. Cristea, C. Dragomirescu, "Process for realisation of a cage adapted to patient for specific acetabular defects in tha revision," UPB Scientific Bulletin, Series D: Mechanical Engineering, vol. 76, pp. 181–192, 2014.

[Lespasio2018] M. J. Lespasio, A. A. Sultan, N. S. Piuzzi, A. Khlopas, M. E. Husni, G. F. Muschler, M. A. Mont, "Hip Osteoarthritis: A Primer," Perm J., vol. 22, 2018, Art no. 17-084, [Online]. Available at: https://doi.org/10.7812/TPP/17-084.

[Mirulla2021] A. I. Mirulla, S. Pinelli, S. Zaffagnini, V. Nigrelli, T. Ingrassia, S. D. Paolo, L. Bragonzoni, "Numerical simulations on periprosthetic bone remodeling: a systematic review," Computer Methods and Programs in Biomedicine, vol. 204, p. 106072, 2021. [Online]. Available at: https://doi.org/10.1016/j.cmpb.2021.106072.

[Paprosky1994] W. Paprosky, P. Perona, J. Lawrence, "Acetabular defect classification and surgical reconstruction in revision arthroplasty: A 6-year follow-up evaluation," The Journal of Arthroplasty, vol. 9, no. 1, pp. 33–44, 1994. [Online]. Available at: https://doi.org/10.1016/0883-5403(94)90135-X.

[Plessers2016] K. Plessers, H. Mau, "Stress analysis of a Burch-Schneider cage in an acetabular bone defect: A case study," Reconstructive Review, vol. 6, no. 1, pp. 37–42, 2016. [Online]. Available at: https://doi.org/10.15438/rr.6.1.141.

[Sződy2017] Sződy R., Kotormán I., Manó S., Csernátony Z., Bagi I., Borbás L., Hatos I., "Csípőprotézis revízióikor alkalmazott „custom made” vápakosár tervezés és készítése, három esetben alkalmazott eljárás," Conference Presentation. VII. Magyar Biomechanikai Konferencia. Szeged, October 6 – 7, 2017.

[Totoribe2018] K. Totoribe, E. Chosa, G. Yamako, X. Zhao, K. Ouchi, H. Hamada, G. Deng, "Acetabular reinforcement ring with additional hook improves stability in three-dimensional finite element analyses of dysplastic hip arthroplasty," Journal of Orthopaedic Surgery and Research, vol. 13, p. 313, 2018. [Online]. Available at: https://doi.org/10.1186/s13018-018-1023-7.

[Vogel2020] D. Vogel, M. Klimek, M. Saemann, R. Bader, "Influence of the Acetabular Cup Material on the Shell Deformation and Strain Distribution in the Adjacent Bone—A Finite Element Analysis," Materials, vol. 13, p. 1372, 2020. [Online]. Available at: https://doi.org/10.3390/ma13061372.

External Figure Sources

Figure 1

[Orthoinfo2020]

Available at:

https://orthoinfo.aaos.org/en/treatment/total-hip-replacement/.

Accessed on: 2023. 09. 14. 16:14

Figure 3

[AO]

Available at:

https://media.aofoundation.org/-/jssmedia/surgery/per30/per30_p280_i460.png?w=400.

Accessed on: 2023. 09. 14. 16:14

[Saumya]

Available at:

https://5.imimg.com/data5/SELLER/Default/2021/1/RE/XP/HL/34019664/cortex-screw-3-5mm-14-tpi-1--500x500.JPG.

Accessed on: 2023.09. 14. 16:15

[Crockarell2009]

Available at:

https://cdn.mdedge.com/files/s3fs-public/Document/September-2017/038090144e.pdf.

Accessed on: 2023. 09. 14. 16:16

[Param]

Available at:

https://parametricsmedical.com/products/traditional-bone/osteosource-cancellous-chips/cancellous-coarse/.

Accessed on: 2021. 06. 10. 10:42